Sensors and Actuators B 141 (2009) 370–380

Contents lists available at ScienceDirect

Sensors and Actuators B: Chemical

journal homepage: www.elsevier.com/locate/snb

Identification and quantification of different vapours using a single polymer chemoresistor and the novel dual transient temperature modulation technique

T. Iwaki [a,b,*], J.A. Covington [b], F. Udrea [c], J.W. Gardner [b]

[a] Research Laboratories, DENSO CORPORATION, Nisshin, Aichi, 470-0111, Japan
[b] School of Engineering, University of Warwick, Coventry, CV4 7AL, UK
[c] Department of Engineering, University of Cambridge, Cambridge CB3 0FA, UK

ARTICLE INFO

Article history:
Received 15 August 2008
Received in revised form 5 May 2009
Accepted 25 June 2009
Available online 9 July 2009

Keywords:
Carbon black/polymer composite
Gas sensor
Micro-hotplate
Temperature modulation

ABSTRACT

This paper presents a novel signal processing technique for a square wave temperature modulated carbon black/polymer composite sensor. The technique consists of only two mathematical operations: summing the off- and on-transients of the conductance signals, and subtracting the steady-state conductance signal. The technique has been verified through its application to a carbon black/polyvinylpyrrolidone composite chemoresistor. Identification of water, methanol and ethanol vapours was successfully demonstrated using the peak time of the resultant curves. Furthermore, quantification of those vapours was found to be possible using the height of the peak heights, which was linearly proportional to concentration. The technique does not require zero-gas calibration and thus is superior to previously reported techniques.

1. Introduction

Although there is a considerable demand for portable, handheld gas or vapour monitors, they have not yet enjoyed great commercial success. The diversity of gases related to air pollution makes it difficult to identify the species and to measure their concentration using a small, low cost instrument. For example, indoor air pollution can be caused by different types of volatile organic compounds (VOCs), such as formaldehyde, benzene, toluene and xylene, emitted from sources inside buildings [1]. Outdoor air pollution can also be caused by various gases such as carbon monoxide, nitrogen oxides, hydrocarbons and again VOCs emitted by automobiles [2].

Currently the most reliable way to identify and quantify hazardous gases is by using expensive, bulky analytical instruments (e.g. gas chromatographs, mass spectrometers and optical spectrometers). There has been significant effort put into reducing the size and the cost of such instruments through miniaturization (e.g. [3]). However, the degree of miniaturization is still limited, due to the nature of the parts required to be replicated, e.g. high voltages, vacuum systems, pumps.

There are two other possible approaches towards developing handheld gas monitors: to either use an array of gas sensors with different sensing materials [4] or temperature modulation of a single gas sensor [5,6]. The feasibility of the former approach has been already demonstrated [4]. However, the development cost in manufacturing 10–20 different types of chemical sensors with guaranteed reliability is high and thus is not suitable for ubiquitous sensing. Concerning the second approach, previous research has been carried out on the temperature modulation of metal oxide chemoresistors [5,6]. Although the identification and quantification were successfully demonstrated, a major issue has to be resolved before commercialization; that is a pre-calibration of the sensors is required for both single gases and importantly their mixtures. This is because the response of high power metal oxide gas sensors is non-linear with gas concentration and thus a simple superposition of the responses for different gases is not always possible [7]. Provided that the identification and quantification of five different types of gases are required, which is a reasonable assumption for environmental gas monitor, pre-calibration has to be carried out for all the possible concentration combinations of those five gases, which makes commercialization difficult.

We recently reported on a novel low power temperature modulation technique using a carbon black/polymer composite chemoresistor sensor capable of identifying and quantifying single vapours by using either the off or on temperature transient of the sensor signal [8,9]. However, the technique was found to have some significant drawbacks as given below:

1. It was not easy to identify the components when mixed, as the curves used are always monotonously increasing (or decreasing). This restricts its application to identifying individual vapours in air and not mixtures.

* Corresponding author. Tel.: +81 561 75 1611; fax: +81 561 75 1193.
E-mail address: TAKAO_IWAKI@denso.co.jp (T. Iwaki).

0925-4005/$ – see front matter © 2009 Elsevier B.V. All rights reserved.
doi:10.1016/j.snb.2009.06.050

2. The technique requires the measurement of the transient conductance of air (zero-gas). This means that it is necessary to measure the zero-gas transients on a regular basis and ideally before each measurement of a vapour—adding complexity and cost to an instrument. Secondly, the sensor cannot be used easily in environments where there is no zero-gas (unless a bottled dry air is included within the unit). This limits the practical application of this method.

In this paper, an improved technique is proposed that overcomes these two limitations and thus significantly enhances the applicability of thermally modulated polymer composite based sensors.

2. Improved signal processing technique

A carbon black/polymer composite is an insulating polymer in which carbon black nanoparticles disperse to form electrical pathways. When the material is exposed to a vapour, the vapour molecules diffuse into the film causing it to swell. This swelling increases the average separation of the conducting nanoparticles and thus decreasing the electrical conductance. In the previous paper, a carbon black/polymer composite film was deposited onto a micro-hotplate and a square wave voltage was applied to a resistive microheater to modulate the temperature [9]. Identification and quantification of water, methanol and ethanol vapours with different concentrations were shown to be possible using either the off- or on-transient of the electrical conductance of the carbon black/polymer composite with two drawbacks described above.

The novel technique proposed in this paper uses both the off- and on-transient responses, unlike the previous technique described in [9]. First, the new technique is explained conceptually, then it is expressed in an analytical form and finally simulations and measurements are given.

The concept of the proposed technique is illustrated in Fig. 1. Here, a square wave temperature modulation of a gas sensor is induced between two temperatures T_1 and T_2 ($T_1 < T_2$) in the presence of a vapour. Fig. 1 (a) and (b) show the conductances of the sensor during the off- and on-transients, respectively. They are aligned so that their temperature changes occur at the same time. Here, $G_{1,\infty}$ and $G_{2,\infty}$ are the steady-state conductance at temperatures T_1 and T_2 of the vapour, respectively. One can note that the thermal response time of the micro-hotplate is smaller than the thermal time constant of the diffusion effect as shown in [9]. The thermal time constant of the diffusion effect for the off-transient is smaller than that for the on-transient because the temperature is lower. Thus, the off- and on-transient curves are not line-symmetric (i.e. The on-transient curve saturates faster than the off-transient one). Next, by simply adding the curves in Fig. 1 (a) and (b), we obtain the curve shown in Fig. 1 (c). A peak is formed as a consequence of the difference in the shapes of the off- and on-transient curves. Although the steady-state conductances $G_{1,\infty}$ and $G_{2,\infty}$ are the final values in the vapour, they will be affected by the baseline drift [9]. However, it is possible to find these values by waiting long enough for the diffusion process to reach equilibrium. Then, by subtracting the curve in Fig. 1 (c) by ($G_{1,\infty} + G_{2,\infty}$), we obtain the curve shown in Fig. 1(d). Thus, one can make the following predictions about the characteristics of the resultant curve:

a. The time of the peak depends only on the diffusion coefficient at T_1 and T_2 (independent of the vapour concentration) and thus is specific to a vapour type.
b. The height of the peak is linearly proportional to the vapour concentration since the amplitudes of both the off- and on-transients are proportional to the vapour concentration.

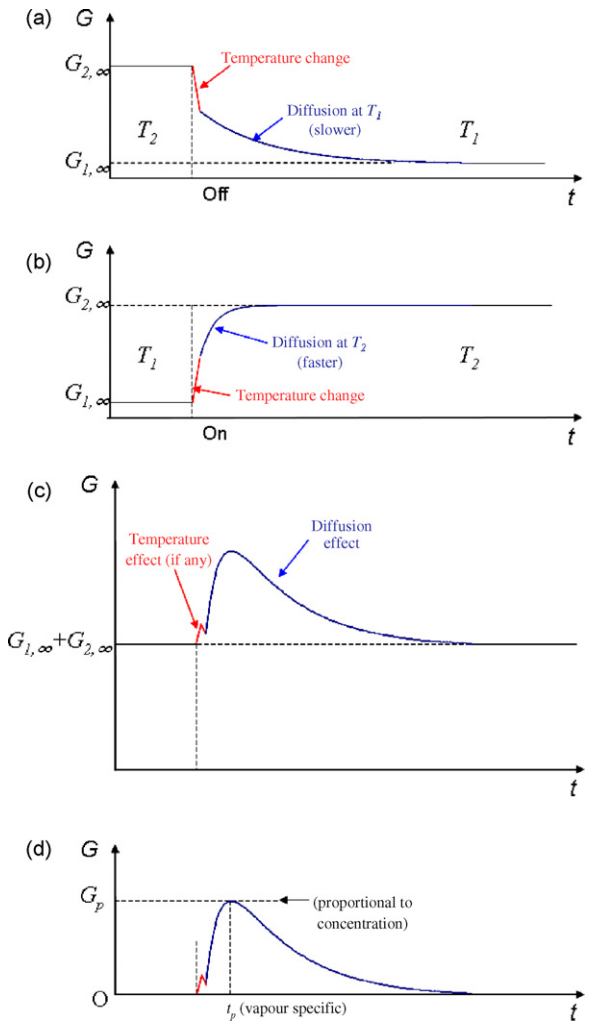

Fig. 1. (a) Sensor conductance of off-transient, (b) sensor conductance of on-transient, (c) sum of off- and on-transients, (d) final peaked curve for identification and quantification (G: conductance, t: time).

c. The curve for a mixture will simply be made of the linear superposition of the individual curves for each vapour, assuming that the species are independent of each other. (Small interactions could be modelled by extension to perturbation or non-linear theory).

To verify the above predictions (a and b), a rigorous mathematical discussion is now given. (Note: Prediction c will not be proven mathematically. This is because the assumption for prediction c is needed for Fick's equation, which our theory starts from. The prediction will however be proven experimentally later).

To calculate the transient conductance for a step temperature decrease from T_2 to T_1 as illustrated in Fig. 2, we first assume that the diffusion of vapour in the polymer simply follows Fick's law [10]

$$\frac{\partial c(x,t)}{\partial t} = D_{T_1}\frac{\partial^2 c(x,t)}{\partial x^2} \quad (0 < x < h) \tag{1}$$

where c is the concentration of the vapour in the polymer, D_{T_1} is the diffusion coefficient of the vapour molecule at T_1, h is the thickness of the film. The initial concentration profile is uniform at T_2 as follows:

$$c(x,0) = c_{\text{polymer}}(T_2) \quad (0 < x < h) \tag{2}$$

where c_{polymer} is the steady-state vapour concentration in the polymer, which is related with the vapour phase concentration c_{vapour}

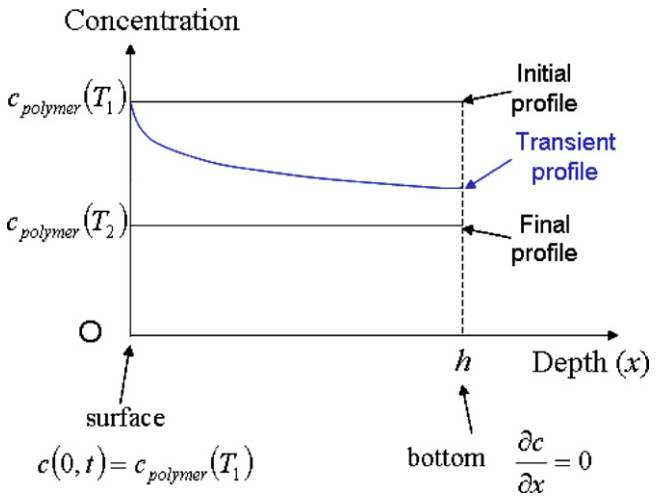

Fig. 2. Illustration of the diffusion problem when temperature decreases instantaneously from T_2 to T_1.

and the partition concentration $K(T)$ as follows:

$$c_{\text{polymer}}(T) = c_{\text{vapour}}K(T) \tag{3}$$

Boundary conditions are set as follows:

$$c(x,0) = c_{\text{polymer}}(T_1) \tag{4a}$$

$$\frac{\partial c}{\partial x} = 0 \quad (x = h). \tag{4b}$$

Eq. (4a) shows that the concentration at the surface of the polymer is independent of time and a constant value of $c_{\text{polymer}}(T_1)$, and Eq. (4b) expresses the condition where there is no flux through the substrate on which the film lies.

Solving Eq. (1) under the conditions of (2), (4a) and (4b), and using the relation (3), we derive the following expression for the vapour molecule concentration profile in the polymer:

$$c(x,t) = c_{\text{vapour}}\left[K(T_1) - \frac{4}{\pi}(K(T_1)-K(T_2)) \times \sum_{m=1}^{\infty}\left[\frac{1}{2m-1}\exp\left(-\frac{\pi(2m-1)^2 D_{T_1}}{4h^2}t\right) \times \sin\left(\frac{\pi}{2h}(2m-1)x\right)\right]\right] \tag{5}$$

The change in local conductivity is assumed to be linearly proportional to the local vapour concentration, hence

$$\Delta\sigma(x) = -Nc(x) \tag{6}$$

where N is a constant. To calculate the fractional difference of the transient conductance G of a thin-film sensor, the local conductance change along a line orthogonal to the film plane is integrated (The mathematical discussion so far is described in more detail in [9]):

$$\frac{\Delta G(t)}{G_{T_1,\text{dry}}} = \frac{G_{T_1}(t) - G_{T_1,\text{dry}}}{G_{T_1,\text{dry}}} = \frac{1}{h}\int_0^h \Delta\sigma(x)dx = -Nc_{\text{vapour}}\left[K(T_1) - \frac{8}{\pi^2}\left\{K(T_1)-K(T_2)\right\} \times \sum_{m=1}^{\infty}\left[\frac{1}{2m-1}\exp\left(-\frac{\pi(2m-1)^2 D_{T_1}}{4h^2}t\right)\right]\right] \tag{7}$$

Thus, the fractional difference of the off-transient is easily found from (7) and may be written as:

(Off-transient)

$$G_{T_1}(t) = G_{T_1,\text{dry}}(t)\left[1 - Nc_{\text{vapour}}\left[K(T_1) - \frac{8}{\pi^2}\left\{K(T_1)-K(T_2)\right\} \times \sum_{m=1}^{\infty}\left[\frac{1}{2m-1}\exp\left(-\frac{\pi(2m-1)^2 D_{T_1}}{4h^2}t\right)\right]\right]. \tag{8}$$

The other transient (temperature increased from T_1 to T_2) is found in the same way and thus the results are written as follows:

(On-transient)

$$G_{T2}(t) = G_{T2,dry}(t)\left[1 - Nc_{\text{vapour}}\left[K(T_2) - \frac{8}{\pi^2}\left\{K(T_2)-K(T_1)\right\} \times \sum_{m=1}^{\infty}\left[\frac{1}{2m-1}\exp\left(-\frac{\pi(2m-1)^2 D_{T2}}{4h^2}t\right)\right]\right] \tag{9}$$

Eqs. (8) and (9) corresponds to the curves shown in Fig. 1 (a) and (b). Simply summing Eqs. (8) and (9) gives:

$$\begin{aligned} G_s(t) = G_{T_1}(t) + G_{T_2}(t) &= \left[G_{T_1,\text{dry}}(t)\left\{1 - Nc_{\text{vapour}}K(T_1)\right\} + G_{T_2,\text{dry}}(t)\left\{1 - Nc_{\text{vapour}}K(T_2)\right\}\right] \\ &+ G_{T_1,\text{dry}}(t)Nc_{\text{vapour}}\frac{8}{\pi^2}\left\{K(T_1)-K(T_2)\right\} \times \sum_{m=1}^{\infty}\left[\frac{1}{2m-1}\exp\left(-\frac{\pi(2m-1)^2 D_{T_1}}{4h^2}t\right)\right] \\ &- G_{T_2,\text{dry}}(t)Nc_{\text{vapour}}\frac{8}{\pi^2}\left\{K(T_1)-K(T_2)\right\} \times \sum_{m=1}^{\infty}\left[\frac{1}{2m-1}\exp\left(-\frac{\pi(2m-1)^2 D_{T_2}}{4h^2}t\right)\right] \end{aligned} \tag{10}$$

which corresponds to the curve in Fig. 1 (c). The peak in Fig. 1 (c) is formed due to the difference of the diffusion coefficients D_{T_1} and D_{T_2}. The equation converges to the following value at the limit when t tends to infinity, or more precisely t is much greater than the diffusion time constants:

$$G_s(\infty) = G_{T_1,\text{dry}}(\infty)\left\{1 - Nc_{\text{vapour}}K(T_1)\right\} + G_{T_2,\text{dry}}(\infty)\left\{1 - Nc_{\text{vapour}}K(T_2)\right\} \tag{11}$$

Since the thermal time constant of the micro-hotplate is much smaller than those of vapour molecule diffusion, the first and second terms of the right hand side of Eq. (10) converge much faster than the third term. Therefore,

$$\begin{aligned} G_s(t) - G_s(\infty) &= Bc_{\text{vapour}}\left[G_{T_1,\text{dry}}(\infty)\sum_{m=1}^{\infty}\left[\frac{1}{2m-1}\exp\left(-\frac{\pi(2m-1)^2 D_{T_1}}{4h^2}t\right)\right] - G_{T_2,\text{dry}}(\infty)\sum_{m=1}^{\infty}\left[\frac{1}{2m-1}\exp\left(-\frac{\pi(2m-1)^2 D_{T_2}}{4h^2}t\right)\right]\right] \\ &(t >> t_m) \end{aligned} \tag{12a}$$

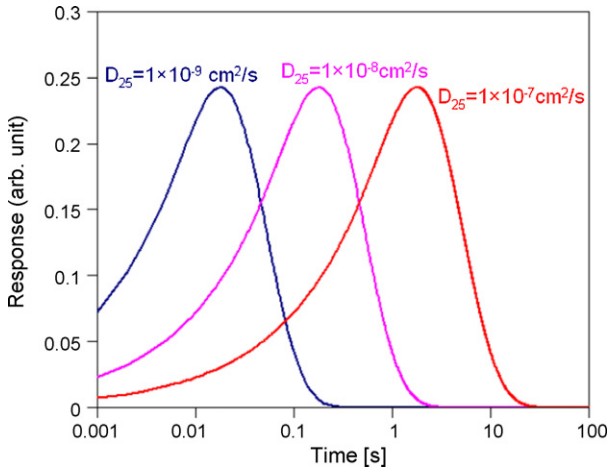

Fig. 3. Simulated response using the improved signal processing technique for three different diffusion coefficients at 25 °C.

$$B \equiv N\frac{8}{\pi^2}\{K(T_1) - K(T_2)\} \tag{12b}$$

where t_m is the response time of the micro-hotplate, and B is a constant. Eq. (12) corresponds to the curve in Fig. 1(d).

Eq. (12) clearly shows that its shape depends only on the diffusion coefficients (apart from parameters that are specific to the sensor i.e. h, $G_{T1,\mathrm{dry}}(\infty)$ and $G_{T2,\mathrm{dry}}(\infty)$) and thus proves prediction (a). The amplitude is proportional to the concentration of the vapour and so proves prediction (b). Later in this paper, $(G_s(t)–G_s(\infty))$ is simply referred to as the"response", and the term "fractional response" denotes a response divided by $(G_1 + G_2)$, which is used when comparing the responses of two sensors with different conductivities.

The theoretical response given by Eq. (12) has been plotted in Fig. 3. Here, the temperature dependence of the diffusion coefficient is assumed to be Arrhenius type (Note: This was shown to be correct for methanol vapour [9]):

$$\frac{D(T_1)}{D_{25}} = \exp\left[-\frac{E_a}{k_B}\left(\frac{1}{T} - \frac{1}{25+273.15}\right)\right] \tag{13a}$$

$$D_{25} = D(25+273.15) \tag{13b}$$

where D_{25} is the diffusion coefficient at 25 °C, E_a is the activation energy, T is the temperature in Kelvin, and k_B is Boltzmann's constant. The following values are used to calculate and plot curves in Fig. 3: $h = 1\ \mu m$, $D_{25} = 1 \times 10^{-7}\ cm^2/s$, 1×10^{-8}, $1 \times 10^{-9}\ cm^2/s$ and $E = 0.40$ eV (measured value for methanol [9]). It was assumed that the temperature steps between 25 °C and 55 °C at $t = 0$ instantaneously. The time axis is plotted in logarithmic scale to differentiate clearly the curves corresponding to $D_{25} = 1 \times 10^{-7}\ cm^2/s$, $1 \times 10^{-8}\ cm^2/s$ and $1 \times 10^{-9}\ cm^2/s$. It demonstrates that species with different diffusion coefficients can be separated theoretically by just the time of their peaks.

Next, the dependence of temperature modulation amplitude was studied. The temperature dependence of the partition coefficient is assumed to be described by the following equation. (Note: This was again shown to be correct for methanol [9]):

$$\frac{K(T)}{K_{25}} = \exp\left[-\frac{\Delta H_0}{R}\left(\frac{1}{T} - \frac{1}{25+273.15}\right)\right] \tag{14a}$$

$$K_{25} = K(25+273.2) \tag{14b}$$

where K_{25} is the partition coefficient at 25 °C, ΔH_0 is the standard enthalpy change for the interaction between the polymer and the vapour molecule, and R is the gas constant. The curves for $h = 1\ \mu m$, $\Delta H_0 = -27.5$ kJ/mol (measured value for methanol vapour [9]) with the temperature modulations of 25 °C ↔ 55 °C, 35 °C ↔ 55 °C and 45 °C ↔ 55 °C are calculated and plotted in Fig. 4(a). Again, it was assumed that the temperature steps at $t = 0$ instantaneously. Relative values (the values for the temperature modulation of 25 °C ↔ 35 °C is defined as unity) of the height of the peaks and FWHM (full width at half maximum) are plotted in Fig. 4(b); indicating that the greater the temperature modulation amplitude, the higher and narrower the peak. Therefore, it is evident that larger temperature amplitudes are preferred for increased accuracy of the technique.

3. Experiments and signal processing

In this section, the new processing technique is applied to both experimental data described in [9] and new data, and discussed in terms of temperature dependence, vapour type and concentration dependence, thickness dependence, mixture effect, and averaging.

3.1. Carbon black/polymer chemoresistor device

Fig. 5 shows a schematic cross section of the chemoresistor used in this work. The CMOS micro-hotplate comprises a silicon nitride/silicon dioxide membrane in which a highly doped single crystal silicon (SCS) resistive heater is sandwiched. The shapes of both membrane and heater were designed to be circular with the radii of 282 and 75 microns, respectively. The electric current was supplied to the microheater via aluminium tracks embedded in the membrane. The electrodes used to measure the electrical conductance of the sensing materials are also made of aluminium onto which Au/Ni were electrodelessly plated (i.e., bump bonded) to make stable ohmic contact to the sensing material. These elec-

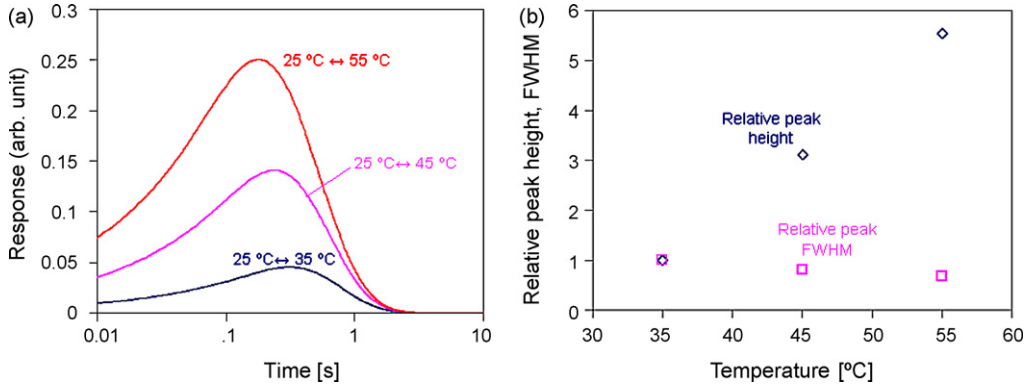

Fig. 4. (a) Simulated temperature dependence of the response of the new processing technique. (b) Simulated relative peak height and FWHM of the response.

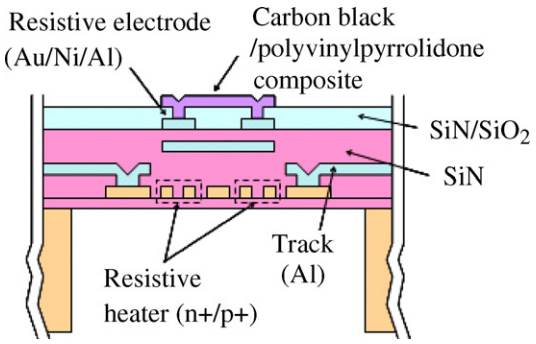

Fig. 5. Schematic cross section of a carbon black/polyvinylpyrrolidone composite chemoresistor employing an SOI–CMOS based single crystal silicon microheater.

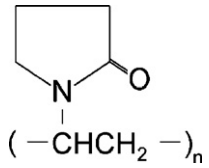

Fig. 6. Structural formula of PVP.

trodes have interdigitated structures with aspect ratios of 16. The micro-hotplate is described in more detail in [11].

Carbon black/polyvinylpyrrolidone (PVP) composite (20 wt% carbon black) was chosen as the sensing material. The PVP used in this work was in powder form with a molecular weight of ca. 40,000 supplied by Sigma–Aldrich (U.K.). The structural formula of PVP is shown in Fig. 6. The polymer contains two atoms with strong electronegativity, i.e., oxygen and nitrogen (electronegativity of oxygen and nitrogen atoms are 3.5 and 3.0 in Pauling's definition) [12]. Therefore, it is expected that the carbon black/PVP composite has a larger sensitivity to polar vapours, such as alcohols, than non-polar vapours. The carbon black nanospheres with a diameter of typically 50–80 nm (Black Pearls 2000) were supplied by Cabot Corporation (USA). The mixture was deposited onto a micro-hotplate using a commercial air brush (HB-BC or HP-CP, Iwata, Japan) through a mask made by microstereolithography. After deposition, heat treatment at 50 °C for 24 h was carried out in an oven to evaporate the solvent and stabilize the sensor resistances. Finally, the sensors were exposed to the flow of dry air at 25 °C for 12 h using an FIA (flow injection analysis) test station (described later). Table 1 lists the resistances, thicknesses, and sheet resistances of the three devices used in these experiments (referred to as PVP2, PVP8 and PVP11) and Fig. 7 shows the photograph of PVP8. The resistances of the film were measured at 25 °C in the dry air environment in the FIA test station. The deposition process of PVP is described in more detail in [9].

3.2. Temperature modulation experiments

Temperature modulation experiments of the three devices (PVP2, PVP8 and PVP11) were performed in a stainless steel chamber with a controlled temperature of 25 °C in a fully automated FIA test station. The temperature of the carbon black/PVP composite film was controlled by applying a voltage to the micro-hotplate. The temperatures used in the experiments were 25 °C, 35 °C, 45 °C and 55 °C that require operating voltages of 0 V, 0.78 V, 1.10 V and 1.35 V, respectively. The accuracy of the temperature modulation amplitude was 0.3 °C. The concentrations of water, methanol and ethanol vapours in the chamber were controlled independently with an uncertainty of only 5%. A constant current of 10 μA was applied to the carbon black/PVP composite film and the voltage was recorded every 10 ms.

Table 1
List of sensors and some film properties.

	Resistance [kΩ]	Thickness [μm]	Sheet resistance [kΩ]
PVP2	4.43	1.9	70.9
PVP8	1.91	6.0	30.6
PVP11	13.65	0.8	218.4

3.3. Temperature dependence

First of all, the results for methanol vapour (concentration: 2710 ppm) with different temperature modulation amplitudes (25 °C ↔ 55 °C, 35 °C ↔ 55 °C, 45 °C ↔ 55 °C) taken in [9] were processed. The sensor used was PVP11. The frequency and duty cycle of the square wave were 50 mHz and 50%, respectively.

Fig. 8 (a) shows the processed data. The origin of the time axis ($t = 0$) was defined as the time when the heater voltage switches to cause temperature off- and on-transients (The temperature changes within 10 ms after the voltage switches [13]). The curves shown are generated by averaging six transients. The curves and their temperature dependence are similar to the theoretical results (Fig. 4 (a)). In fact, the measured temperature dependence of the relative height and FWHM of the peaks is very close to that obtained through simulations as shown in Fig. 8 (b). The simulations are based on the experimental values of methanol to describe the temperature dependence, and thus can be compared with the experiments, suggesting that the theory is valid.

The shapes of the curves are different from the simulations at the left hand side tail region. This is because the sampling period of each curve is 10 ms and hence the tail regions were not measured accurately.

3.4. Vapour type and concentration dependence

Temperature modulation (between 25 °C and 55 °C) experiments of device PVP11 were performed in the presence of single vapours (water, methanol and ethanol) in air and the results processed using the new technique. The frequency and duty cycle of the square wave were 50 mHz and 50% for water and methanol, and 1.67 mHz and 50% for ethanol, respectively.

The results are shown in Fig. 9. The curves for water and methanol vapour are averages of 30 transients and that for ethanol vapour are an average of three transients. As predicted, each vapour

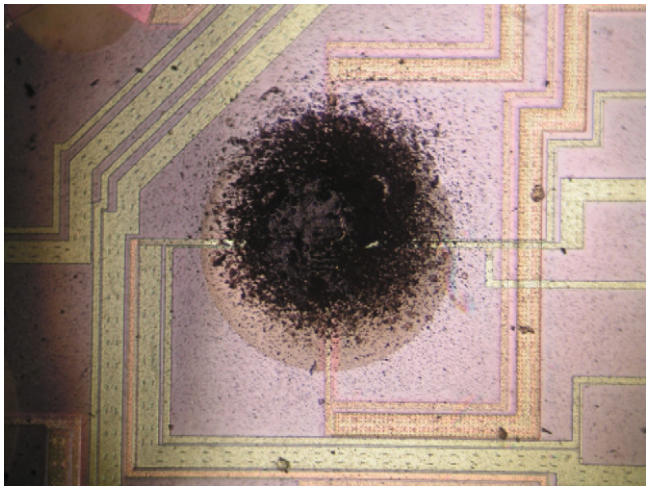

Fig. 7. Photograph of the chemoresistor device (PVP8).

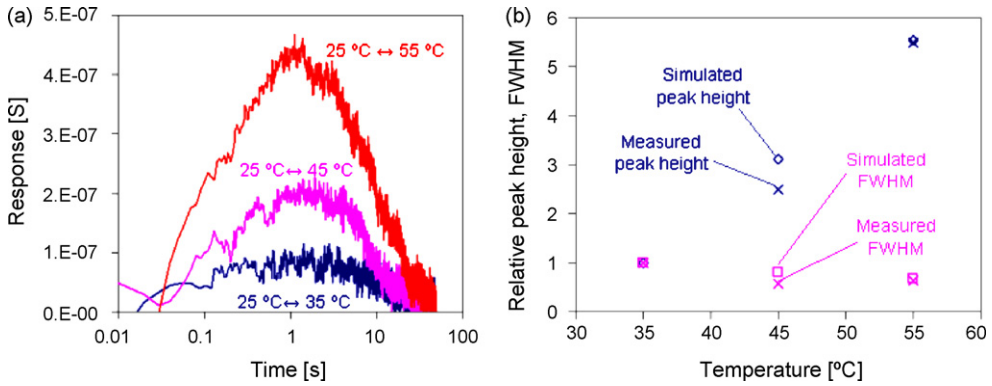

Fig. 8. (a) Characteristic behaviour in methanol (concentration: 2710 ppm) for different temperature modulation amplitudes. (b) Measured relative peak height and FWHM of the response in methanol vapour (concentration: 2710 ppm) with different temperature modulation amplitudes, as compared with the simulations.

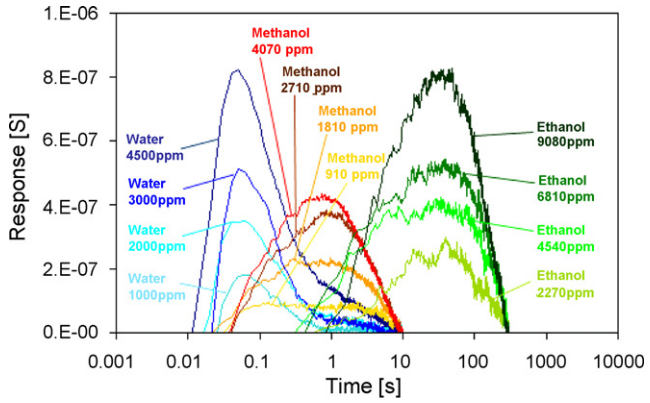

Fig. 9. Responses to water, methanol and ethanol vapours of different concentrations.

is separated out clearly using the difference of their peaks in time (water: 50 ms, methanol: 1 s, ethanol 30 s). This is a reasonable result indicating that the species with highest molecular mass has a highest diffusion coefficient (molecular mass of water, methanol and ethanol are 18, 32 and 46, respectively). The height of the peaks, shown in Fig. 9, increases when the vapour concentration increases–as the theory predicts. Fig. 10 plots the sensor responses of all the vapours (water, methanol and ethanol) at different concentrations with linear regression lines and *f*ared values. The experimentally obtained responses vs. concentration data are fitted well with regression lines, again as the theory predicts. However, the linearity should be confirmed by further experiments especially for methanol vapour considering the relatively low *R*-squared value of 0.893. According to Eq. (12), the linear relationship is expected only in the concentration range where the partition coefficient is independent of the concentration (i.e. Eq. (3)). It should be noted that the linearity will deteriorate at higher concentrations where Eq. (3) becomes invalid.

3.5. Thickness dependence

Temperature modulation (between 25 °C and 35 °C) experiments of the devices PVP8 (thickness: *ca.* 6 μm) and PVP11 (thickness: *ca.* 0.8 μm) were performed in the presence of different concentrations of water vapour. The frequency and duty cycle of the square wave were 10 mHz and 50%. The results were processed using the new technique.

Fig. 11 shows the results. The curves are the averages of 30 transients. The thicker film has a 60× greater peak time (3 s) than the thinner film (50 ms). This is a reasonable value as the peak time should be proportional to the square of the ratio of thickness (i.e. $(6/0.8)^2 = 56$) and considering the significant uncertainty in the thickness measurements (described in [9]).

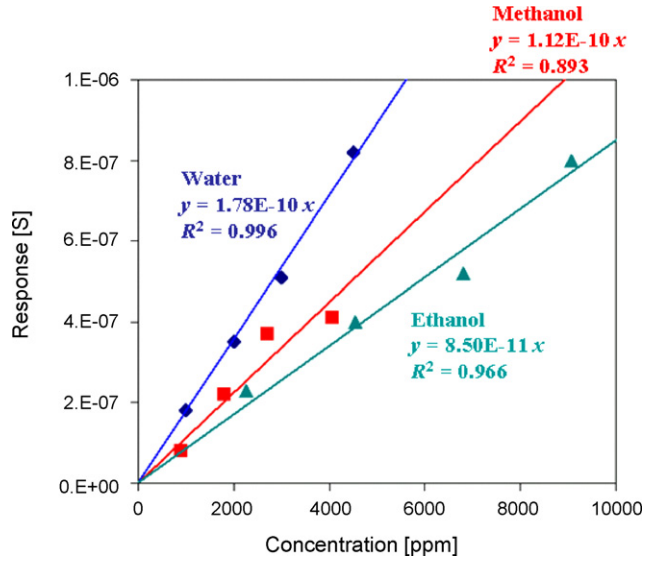

Fig. 10. Concentration dependence of responses to water, methanol and ethanol vapours in air.

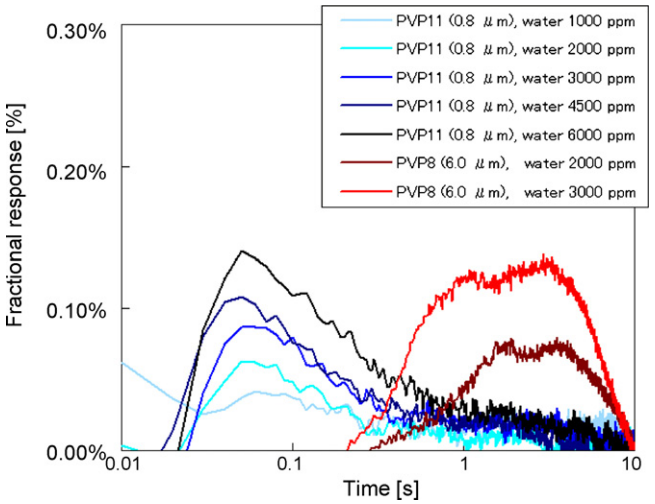

Fig. 11. Thickness dependence of the fractional response to water vapour with different concentrations.

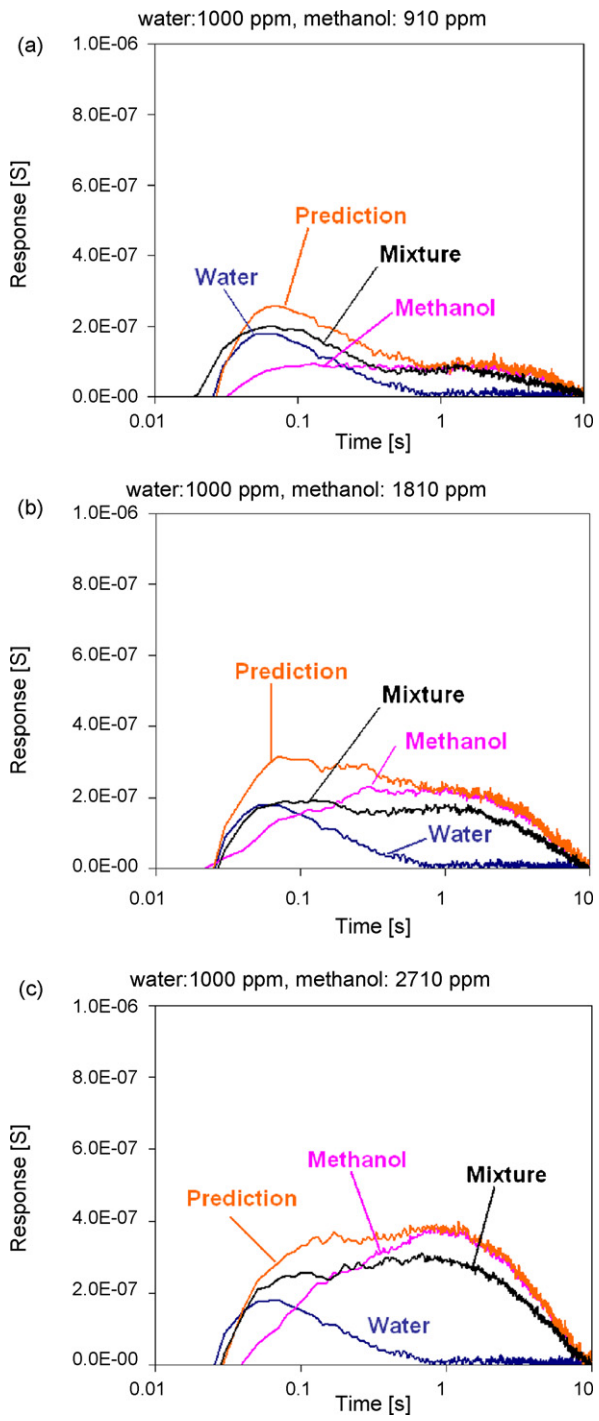

Fig. 12. Results for mixtures of water concentrations of 1000 ppm and methanol concentrations of (a) 910 ppm, (b) 1810 ppm, (c) 2710 ppm.

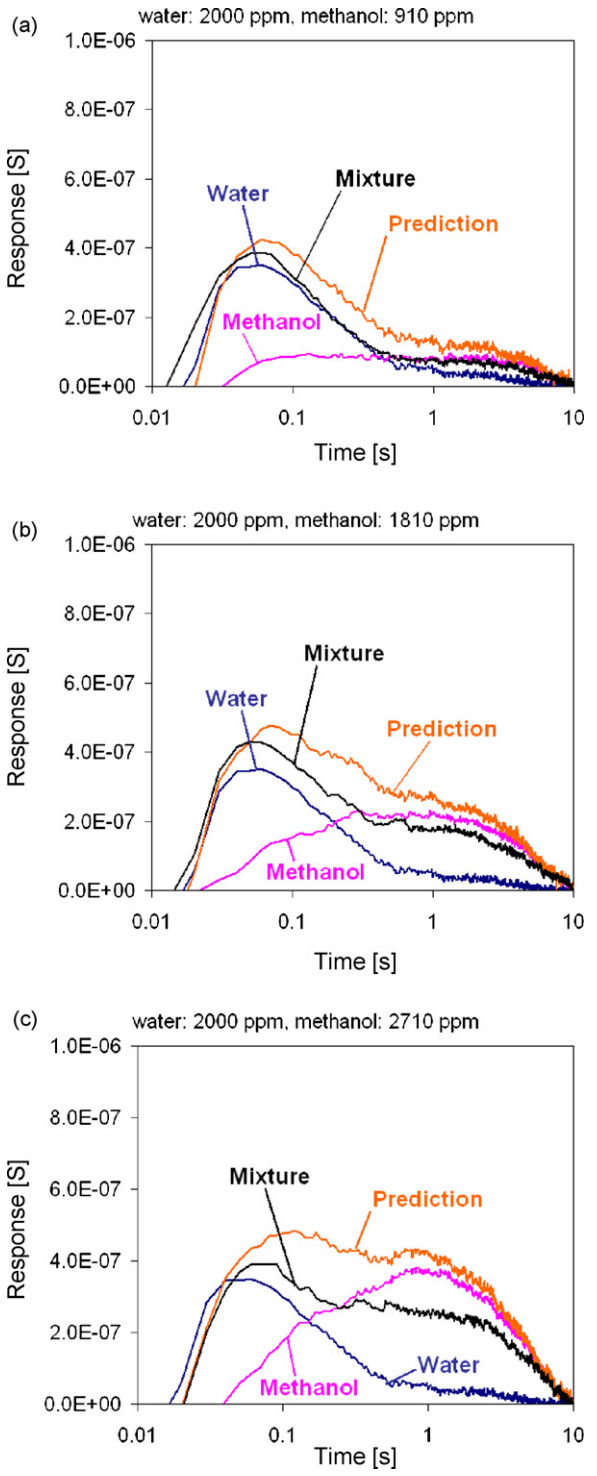

Fig. 13. Results for mixtures of water concentration of 2000 ppm and methanol concentrations of (a) 910 ppm, (b) 1810 ppm, (c) 2710 ppm.

3.6. Mixture effect

Temperature modulation (between 25 °C and 55 °C) experiments of mixtures (water and methanol) were performed. The results were processed using this new technique. The device used was PVP11. The frequency and duty cycle of the square wave were 50 mHz and 50%.

The results are shown in Figs. 12–14 with each curve the average of 30 transients. Results correspond to water and methanol concentrations of (1000 ppm, 910 ppm), (1000 ppm, 1810 ppm), (1000 ppm, 2710 ppm), (2000 ppm, 910 ppm), (2000 ppm, 1810 ppm), (2000 ppm, 2710 ppm), (3000 ppm, 910 ppm), (3000 ppm, 1810 ppm) and (3000 ppm, 2710 ppm) in air, respectively. These figures show both the resultant curves of mixtures and single vapour curves of water and methanol with the corresponding concentrations. The single vapour results were superimposed to predict the curve of the mixtures and plotted as "prediction". It was found that the resultant curves of mixtures are similar to the predicted curves, though there is a tendency that the predicted curves are higher than the experimental ones. The

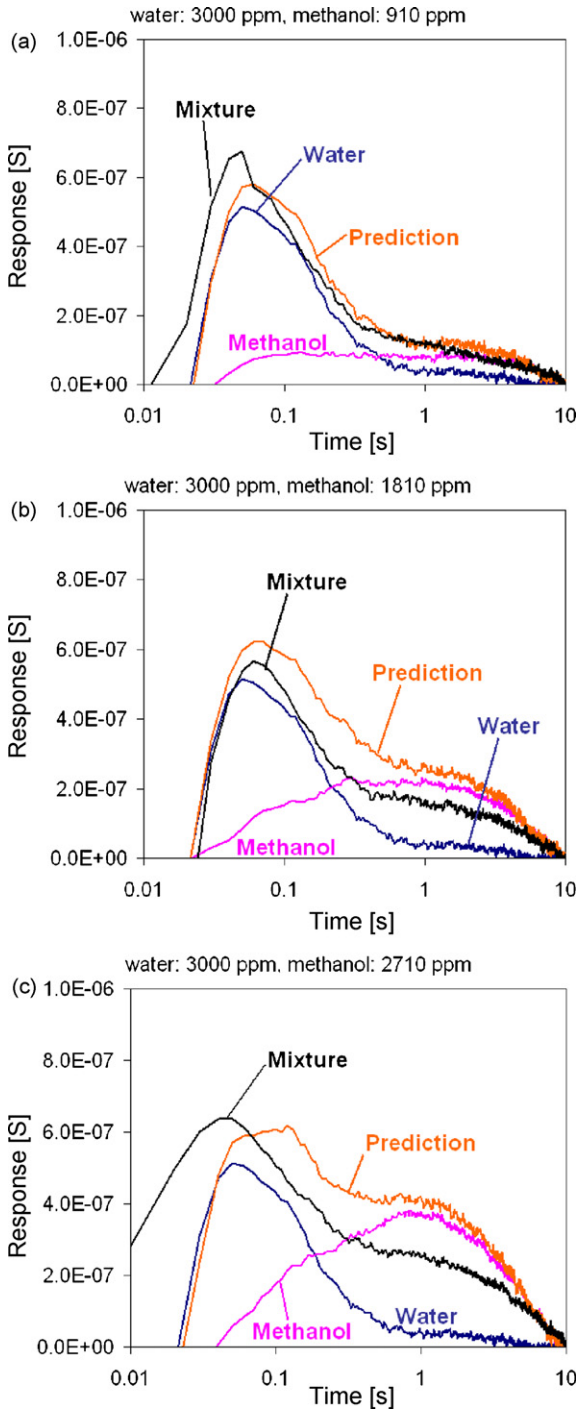

Fig. 14. Results for mixtures of water concentration of 3000 ppm and methanol concentrations of (a) 910 ppm, (b) 1810 ppm, (c) 2710 ppm.

precise cause of this tendency is not understood but might be due to experimental errors.

Quantification of each vapour (water and methanol) was also carried out using the results shown in Figs. 12–14. The concentration of a species in a mixture is calculated by simply subtracting the value of the peak at the time of the species by the sum of the values of the other species at the same point. For example, the concentration of the water in a mixture is calculated by subtracting a value of the mixture by that of methanol at 50 ms as shown in Fig. 15. Fig. 16(a) and Table 2 show the results of quantification of water in mixtures with methanol,and Fig. 16 (b) and Table 3 vice

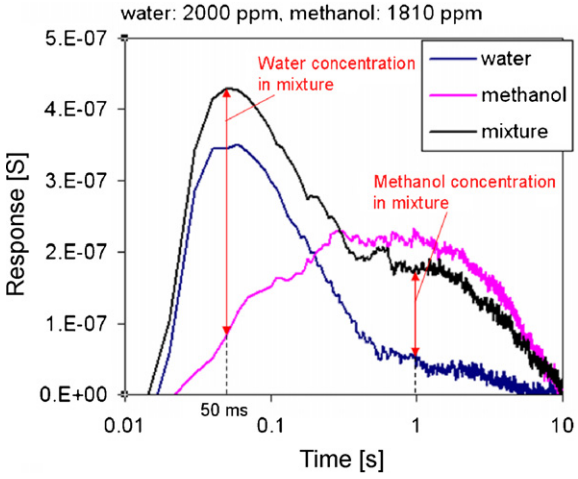

Fig. 15. Calculation of the concentration of each vapour in a mixture.

Table 2
Regression lines for water vapour sensing in mixtures of water and methanol vapours.

	Methanol 0 ppm	Methanol 910 ppm	Methanol 1810 ppm	Methanol 2710 ppm
Equation	$y = 1.000\,x$	$y = 1.079\,x$	$y = 0.8703\,x$	$y = 1.007\,x$
R-squared	0.9956	0.9094	0.9190	0.9471

versa. It was shown that water can be quantified without affected by the presence of methanol. However, methanol cannot be quantified properly with some prediction error: higher water vapour concentration causes a decrease in the predicted methanol concentration. This could be due to experimental errors, but a more likely explanation is given in the next section.

3.7. Averaging

In order to determine the lower detection limit of the sensor, the number of curves that had to be averaged to reduce the noise level to less than 5% was investigated. The temperature modulation (between 25 °C and 55 °C) results of the device PVP11 in the presence of 3000 ppm of water were used for this purpose. Fig. 17(a) and (b) show the response of (a) after averaging 30 raw data signals (thus the same curve as the one in Fig. 9), and (b) the 30 raw data signals. The standard deviation (or the mean square error) of the curves in Fig. 17 (b) at 50 ms (peak time for water) was calculated to be 5.3×10^{-8} S or 10.4% of the peak height. The noise is known to be proportional to the inverse of the square root of the number of samples averaged [14]. Therefore, the number of averaged curves needed to reduce the error to be less than 5% for 3000 ppm water vapour is calculated to be $(10.4\%/5\%)^2 = 4.3$. Since the concentration is linearly proportional to the signal, the following equation is found:

$$n_{5\%} = \frac{3.9 \times 10^7}{c_{\text{water}}^2} \tag{15}$$

where $n_{5\%}$ is the number of curves needed to reduce the measurement error to 5% and C_{water} is the water concentration. Thus to

Table 3
Regression lines for methanol vapour sensing in mixtures of water and methanol vapours.

	Water 0 ppm	Water 1000 ppm	Water 2000 ppm	Water 3000 ppm
Equation	$y = 1.000\,x$	$y = 0.8659\,x$	$y = 0.6899\,x$	$y = 0.6478\,x$
R-squared	0.8930	0.9608	0.9366	0.9376

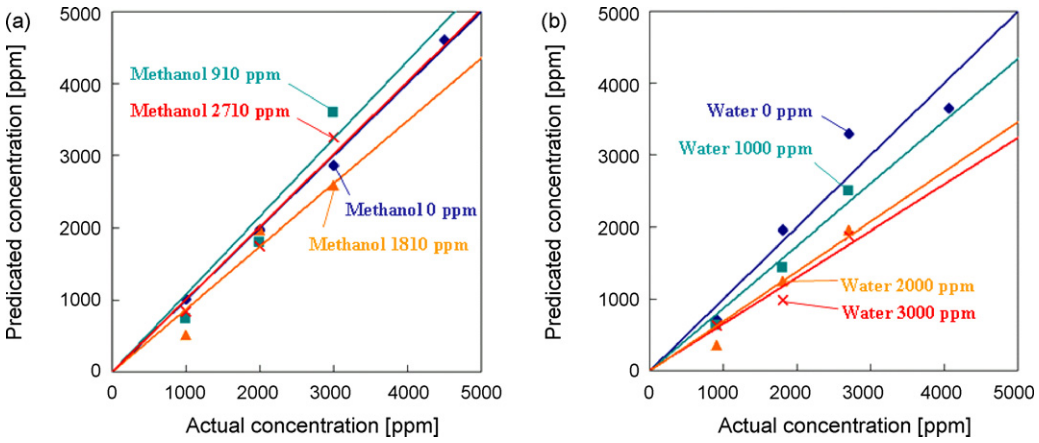

Fig. 16. (a) Results for water vapour sensing in mixtures of water and methanol vapours. (b) Results for methanol vapour sensing in mixtures of water and methanol vapours.

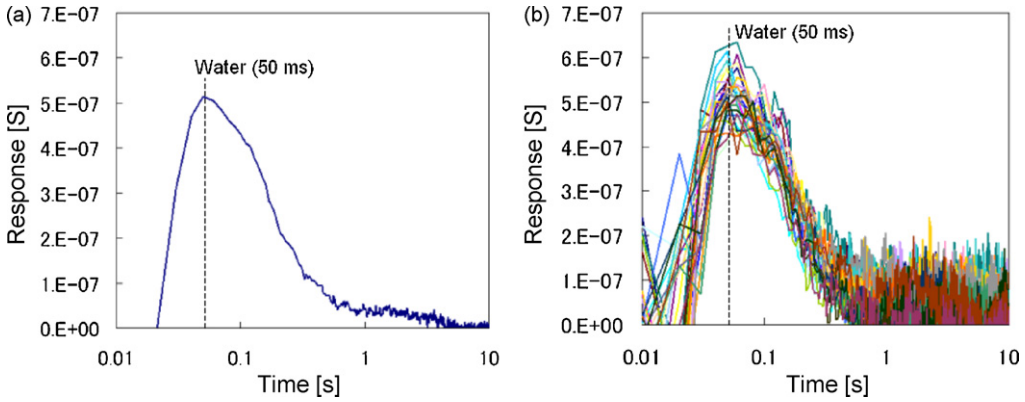

Fig. 17. Response to 3000 ppm of water (a) after averaging 30 raw data signals and (b) 30 raw data signals.

detect 100 ppm of water, averaging of more than 1000 curves are required.

It should be noted that the relatively low signal-to-noise ratio reported in this paper may be due to the fact that the output signal of the sensors were transferred to the data acquisition PC without being amplified. Therefore the noise, and thus the number of averaging required, may be reduced significantly by, for example, integrating the detection circuitry with the sensor and amplifying the signal-on-chip.

4. Discussions

The technique proposed is supported by an analytical model and predicts (a) the response of the polymer sensor is linearly proportional to the vapour concentration, and (b) linear superposition of responses for each vapour in a mixture is possible. These characteristics make vapour/gas detection in a simple mixture relatively straightforward. The advantage of (b) superposition is particularly attractive. Suppose that a vapour/gas sensor is sensitive to five different vapours/gases then unless superposition is possible, one would be required to pre-calibrate the sensor response to all the possible combination of concentrations. For example, assuming that five different concentrations are needed for one vapour/gas, $5^5 = 3125$ pre-measurements (covering all the possible combinations) have to be carried out. However, if superposition is possible, only $5 \times 5 = 25$ pre-measurements (for single vapour/gases) are sufficient, as the response to mixtures can easily be predicted by superposition. Since none of the temperature modulation techniques for metal oxide sensors published previously allow superposition [5,15,16], it is believed that our proposed technique is superior. In addition, it has to be noted that this technique does not rely upon any chemical reactions but relies only on physical mechanisms of linear diffusion and polymer swelling, and thus may offer better long-term reliability.

The linearity of the proposed technique was experimentally demonstrated (Fig. 10) over the concentration range used here. These results also agree with Lewis's work that claims the linearity of the steady-state response of this type of sensors (e.g. [17]). However, the superposition was not clearly shown to be possible. Although this may be due to the experimental errors, the following discussion is given assuming that the results shown in Fig. 16 indicate that a linear superposition is problematic. One possible explanation of this is that the second solvent (e.g. methanol) is enhancing the diffusion of the first solvent (e.g. water) as published in [18]. It is believed that there is a way to obviate this issue. This is because the vapour molecules should not affect each other as long as their concentrations are low. There are ways to reduce the concentrations in the polymers at the expense of sensitivity:

1. Increasing the temperature (e.g. From 25 °C ↔ 55 °C to 35 °C ↔ 65 °C)
2. Using less sensitive polymers (PVP was chosen as it has the highest concentration to methanol in [19]. By choosing for example poly(styrene), the sensitivity decreases by the factor of 0.05)

However many practical applications involve the detection of lower concentrations of vapours than tested here and so this would mean that the system would be naturally more linear. The additive behaviour of steady-state response of carbon black/poly(ethylene-

co-vinyl acetate) to benzene and heptane at low concentrations ($0.005 < P/P_0 < 0.015$, where P_0 is the vapour pressure of the analyte) supports this idea [17].

It should be stated that the response of the sensor is relatively slow. For example, the peak for ethanol is at 30 s and it was necessary to wait until 300 s to form the peak. However, the response time of this sensor is strongly dependent upon film thickness (i.e. proportional to the square of the thickness) as experimentally demonstrated using water vapour in Section 3.5, because the phenomenon is governed by linear diffusion. Therefore, it is expected that the response time (i.e. time needed to form the peak) will decrease to less than 1 s by using a film about 8% of the thickness (Note: However, decreasing the film thickness may deteriorate some of the properties of the sensors e.g. signal-to-noise ratio and long term stability. The thickness of the film should be optimized experimentally considering these negative effects).

It should be stated that the concentration ranges for methanol (910–4070 ppm) and ethanol (2270–9080 ppm) used in this paper were higher than the legal exposure limits of methanol and ethanol (200 ppm and 1000 ppm in UK [20]). Also the concentration range of 1000 ppm–4500 ppm for water corresponds to the relative humidity of 4.3–19.5% at 20 °C, which does not cover the possible maximum relative humidity (i.e. 100%). Therefore, when applying the proposed technique into handheld gas monitors, experiments that cover the above concentration ranges (possibly with different types of polymers for optimization) will be needed.

5. Conclusions

In this paper, a novel signal processing technique for a carbon black/polymer composite sensor is proposed, modelled, and demonstrated. The technique is simple, that is summing the off- and on-transient conductances and subtracting the steady-state conductance value from the resulting curve. It is theoretically predicted that the peak time is specific to the type of vapour while the height of the peak of the resultant curve is linearly proportional to the vapour concentration. Therefore different vapours can be identified and their concentration predicted. It is also predicted that the resultant curve for a mixture of vapours can be obtained by a superposition of the curves of its constituents. Since the resultant curve of this improved technique features conductance peaks and unlike other techniques does not rely on zero-gas baseline values, this technique should have a more widespread application and ultimately offer a lower cost solution.

The experimental results taken were processed using the new technique with the following observations:

1. The larger temperature modulation amplitude makes the peak height larger and FWHM narrower for methanol vapour. Therefore higher temperature modulation is desirable.
2. Water, methanol and ethanol vapours have their specific peak time i.e. 50 ms, 1 s and 30 s, respectively, for the 0.8 μm thick PVP film, and thus can be separated out easily.
3. The response is linearly proportional to the vapour concentration for water, methanol and ethanol in the concentration range tested (water: 1000–4500 ppm, methanol: 910–4070 ppm, ethanol: 2270–9080 ppm).
4. A thicker film has a longer peak time (proportional to the square of the thickness) for water.

Therefore, it is concluded that this new technique can readily identify and quantify single vapours. This means that the technique is superior to other temperature modulation techniques reported elsewhere, e.g. for metal oxide based sensors. The technique was also applied to mixtures of water and methanol with different concentrations. Water vapour was quantified properly without interference from methanol vapour, which is a promising result supporting superposition and hence the main advantage of the proposed technique. However, methanol vapour quantification was difficult at high water vapour concentration (i.e. >1000 ppm). There will probably be a maximum concentration for each vapour that allows the superposition, but more experimental work is needed to verify this statement. Finally, we believe that our SOI–CMOS micro-hotplate sensor with this signal processing technique will lead to an on-chip analytical instrument with embedded software.

References

[1] United States Environmental Protection Agency (EPA), Indoor air facts No. 4 (revised), sick building syndrome, 1991.
[2] UK air quality archive, http://www.airquality.co.uk/archive/index.php, accessed on 15th November 2007.
[3] C.M. Matzke, R.J. Kottenstette, S.A. Casalnuovo, G.C. Frye-Mason, M.L. Hudson, D.Y. Sasaki, R.P. Manginell, C.C. Wong, Microfabricated silicon gas chromatographic microchannels: fabrication and performance, Proceedings of SPIE 3511 (1988) 262–282.
[4] E.J. Severin, B.J. Doleman, N.S. Lewis, An investigation of the concentration dependence and response to analyte mixtures of carbon black/insulating organic polymer composite vapor detectors, Analytical Chemistry 72 (4) (2000) 658–668.
[5] A. Heilig, N. Bârsan, U. Weimar, M. Schweizer-Berberich, J.W. Gardner, W. Göpel, Gas identification by modulating temperatures of SnO_2-based thick film sensors, Sensors and Actuators B 43 (1997) 45–51.
[6] E. Llobet, R. Ionescu, S. Al-Khalifa, J. Brezmes, X. Vilanova, X. Correig, N. Barsan, J.W. Gardner, Multicomponent gas mixture analysis using a single tin oxide sensor and dynamic pattern recognition, IEEE Sensors Journal 1 (3) (2001) 207–213.
[7] K. Ihokura, J. Watson, The Stannic Oxide Gas Sensor, Principles and Applications, CRC Press, Boca Raton, 1994.
[8] T. Iwaki, J.A. Covington, J.W. Gardner, Identification of vapours using a single carbon black/polymer composite sensor and a novel temperature modulation technique, Proceedings of IEEE Sensors October 2007, 2007, pp. 1229–1232.
[9] T. Iwaki, J.A. Covington, J.W. Gardner, Identification of different vapours using a single temperature modulated polymer sensor with a novel signal processing technique, IEEE Sensors Journal 9 (4) (2009) 314–328.
[10] S.M. Briglin, N.S. Lewis, Characterization of the temporal response profile of carbon black-polymer composite detectors to volatile organic vapors, Journal of Physical Chemistry B 107 (2003) 11031–11042.
[11] T. Iwaki, J.A. Covington, F. Udrea, C.S. Blackman, I.P. Parkin, SOI-CMOS based single crystal silicon micro-heaters for gas sensors, Proceedings of IEEE Sensors October 2006, 2006, pp. 460–463.
[12] D.R. Lide, Handbook of Chemistry & Physics, 87th edition 2006–2007, CRC, 2006.
[13] P.K. Guha, S.Z. Ali, C.C.C. Lee, F. Udrea, W.I. Milne, T. Iwaki, J.A. Covington, J.W. Gardner, Novel design and characterisation of SOI CMOS micro-hotplates for high temperature gas sensors, Sensors and Actuators B 127 (2007) 260–266.
[14] J.R. Taylor, An introduction to error analysis: the study of uncertainties in physical measurements, University Science Books, Sausalito, 1997.
[15] E. Llobet, R. Ionescu, S. Al-Khalifa, J. Brezmes, X. Vilanova, X. Correig, N. Bârsan, J.W. Gardner, Multicomponent gas mixture analysis using a single tin oxide sensor and dynamic pattern recognition, IEEE Sensors Journal 1 (3) (2001) 207–212.
[16] E. Llobet, J. Brezmes, R. Ionescu, X. Vilanova, S. Al-Khalifa, J.W. Gardner, N. Bârsan, X. Correig, Wavelet transform and fuzzy ARTMAP-based pattern recognition for fast gas identification using a micro-hotplate gas sensor, Sensors and Actuators B 83 (2002) 238–244.
[17] E.J. Severin, B.J. Doleman, N.S. Lewis, An investigation of the concentration dependence and response to analyte mixtures of carbon black/insulating organic polymer composite vapour detectors, Analytical Chemistry 72 (2000) 658–668.
[18] J.S. Vrentas, J.L. Duda, H.-C. Ling, Enhancement of impurity removal from polymer films, Journal of Applied Polymer Science 30 (1985) 4499–4516.
[19] M.C. Lonergan, E.J. Severin, B.J. Doleman, S.A. Beaber, R.H. Grubbs, N.S. Lewis, Array-based vapor sensing using chemically sensitive, carbon black-polymer resistors, Chemistry of Materials 8 (1996) 2298–2312.
[20] Business Link, http://www.businesslink.gov.uk, accessed on 5th May 2009.

Biographies

Takao Iwaki received his BSc and MSc degrees in Physics from Tokyo University in 1995 and 1997 respectively and his PhD degree in Engineering from Warwick University in 2008. He is with the Research Laboratories of DENSO CORPORATION since 1997. His research interests include gas sensors and microsystem technology. He is a member of the Institute of Electrical Engineers of Japan (IEEJ).

James Covington (BEng MRes PhD MIET) is presently an Associate Professor in the School of Engineering at the University of Warwick. He received his BEng 1996 in

Electronic Engineering and remained there receiving his PhD 2000. His PhD was on the development of CMOS and SOI–CMOS gas sensors for room temperature and high temperature operation. He worked as a research fellow for both Warwick University and Cambridge University on the development of gas and chemical sensors and was appointment as a lecturer in 2002. Current research interests focus on the development of silicon devices with novel materials using CMOS and SOI ASIC technology (nose-on-a-chip), and biologically inspired neuromorphic devices with applications based on environmental and biomedical engineering.

Florin Udrea received an MSc degree in microelectronics from the Politehnica University of Bucharest, Bucharest Romania, in 1991, a second masters in smart sensors from the University of Warwick, UK, in 1992 and a PhD degree in power devices from the University of Cambridge, Cambridge, UK, in 1995. Since October 1998, he has been a reader with the Department of Engineering, University of Cambridge, UK. He was an advanced EPSRC Research Fellow from August 1998 to July 2003 and, prior to this, a College Fellow in Girton College, University of Cambridge. He is currently leading a research group in power semiconductor devices and solid-state sensors that has won an international reputation during the last 10 years. In August 2000, he cofounded, with Prof. G. Amaratunga, Cambridge Semiconductor (Cam-Semi), Cambridge, UK, a start-up company in the field of power integrated circuits, where he is currently the Technical Director. He published over 150 papers in journals and international conferences. He holds 22 patents in power semiconductor devices and sensors. Dr. Udrea won six Best Paper Awards as first author in IEEE international conferences.

Julian Gardner (BSc PhD DSc FREng FIEE SMIEEE) is Professor of Electronic Engineering in the School of Engineering at Warwick University. He is author or co-author of over 400 technical papers and patents as well as six technical books in the area of microsensors and machine olfaction. He is Series Editor for a books series by Wiley-VCH. He is a fellow of the IEE and senior member of the IEEE and has served on many advisory panels on sensors, e.g. for EPSRC, DTI and IEE Professional Network on Microsystems and Nanotechnology. His research interests include the modelling of silicon microsensors, chemical sensor array devices, biomimetic MEMS devices and electronic noses. He has worked with over 20 companies in the past 15 years developing commercial e-nose instruments and a consultant for various companies. He is also Head of the Sensors Research Laboratory and Director of the Centre for Cognitive & Neural Systems. He was elected a Fellow of the Royal Academy of Engineering in 2006 and awarded the JJ Thomson Medal for Outstanding Achievement in Electronics by the Institute of Engineering & Technology in 2007.